STATE OF NEW MEXICO
BEFORE THE WATER QUALITY CONTROL COMMISSION

In the Matter of:	)	
PROPOSED AMENDMENT TO 20.6.2 NMAC (Copper Rule)	)	**No. WQCC 12-01(R)**

EXHIBIT SCOTT – D-34

10. Shinn, E. A., "Burrowing in Recent Lime Sediments of Florida and the Bahamas," *Journal of Paleontology*, Vol. 42, No. 4, 1968, pp. 879–894.
11. Sowers, G. F., "Failures in Limestones in Humid Subtropics," *Journal of the Geotechnical Engineering Division*, ASCE, Vol. 101, No. GT8, Proc. Paper 11521, Aug., 1975, pp. 771–787.
12. Sowers, G. F., closure to "Failures in Limestones in Humid Subtropics," *Journal of the Geotechnical Engineering Division*, ASCE, Vol. 103, No. GT7, Proc. Paper 13025, July, 1977, pp. 807–813.
13. Teng, W. C., *Foundation Design*, Prentice-Hall, Inc., Englewood Cliffs, N.J., 1962, pp. 131–134.
14. Webb, D. L., "Settlement of Structures on Deep Alluvian Sandy Sediments in Durban, South Africa," *Proceedings*, Conference on In-Situ Behavior of Soil and Rock, Institution of Civil Engineers, 1969, pp. 181–188.
15. Westergaard, H. M., and Slater, A., "Moments and Stresses in Slabs," *Proceedings*, American Concrete Institute, Vol. 17, 1921.

Shear Strength of Rockfill

By Nick Barton[1] and Bjørn Kjærnsli[2]

Introduction

An important question which arises during stability analysis of rockfill dams is the relative frictional resistance of the rockfill and the underlying rock foundation interface. Attempts to estimate the shear strength of smooth, ice-polished interfaces has led to an examination of the related shear behavior of rock joints. It is found that rockfill, interfaces, and rock joints have several features in common, including dilatant behavior under low effective normal stress, and significant crushing of contact points with reduced dilation at high stress. In each case failure is resisted by strongly stress dependent friction angles. As an example, the peak drained friction angle ϕ' of rockfill near the base of a high dam may be as low as 35°, while close to the toe the same rockfill might exhibit a value of ϕ' as high as 60°. Similar stress dependency is observed with rock joints and interfaces.

In this article it is shown how the value of ϕ' for rockfill can be estimated from knowledge of the following parameters: (1) The uniaxial compressive strength of the rock; (2) the d_{50} particle size; (3) the degree of particle roundedness; and (4) the porosity following compaction. The degree of particle roundedness and the porosity determine the magnitude of the structural component of strength. This component increases shear resistance in much the same way as interlocking asperities on a rough joint surface. The structural component of strength is strongly stress dependent. It is added to the basic angle of friction ϕ_b of flat nondilatant, i.e., sawn, surfaces of the rock to obtain ϕ'.

The methods developed here are of a simple practical nature, and allow a dam designer to obtain a preliminary estimate of the peak drained friction angle of rockfill, whether it consists of angular quarried rock, moraine, or well-rounded fluvial gravels. Simple large scale tilt tests of in-place rockfill are suggested for checking the shear strength in different lifts of a dam, during construction.

[1]Sr. Staff Consultant, Terra Tek, 420 Wakara Way, Salt Lake City, Utah 84108; formerly Sr. Engr., Dam and Rock Group, Norwegian Geotechnical Inst., Oslo, Norway.
[2]Chf. Engr., Dam and Rock Group, Norwegian Geotechnical Inst., Oslo, Norway.

Note.—Discussion open until December 1, 1981. To extend the closing date one month, a written request must be filed with the Manager of Technical and Professional Publications, ASCE. Manuscript was submitted for review for possible publication on December 11, 1980. This paper is part of the Journal of the Geotechnical Engineering Division, Proceedings of the American Society of Civil Engineers, ©ASCE, Vol. 107, No. GT7, July, 1981. ISSN 0093-6405/81/0007-0873/$01.00.

A practical method for describing the peak shear strength of three typical classes of rock joints is shown in Fig. 1 (2). The general equation is as follows:

$$\tau = \sigma_n' \tan\left[\mathrm{JRC}\cdot\log\left(\frac{\mathrm{JCS}}{\sigma_n'}\right) + \phi_r\right] \quad \text{(1)}$$

in which τ = peak shear strength; σ' = effective normal stress; JRC = joint roughness coefficient; JCS = joint wall compression strength; and ϕ_r = residual angle of friction.

JRC.—The joint roughness coefficient is a dimensionless number, approximately equivalent to the ratio of roughness amplitude and sample length. Completely planar smooth joints, or sawn surfaces have JRC equal to zero. The most reliable method of measuring JRC is to conduct tilt tests, preferably with rock blocks of natural size containing through-going joints. Sliding occurs due to the effect of gravity on the upper block. The JRC is back-calculated by rearrangement of Eq. 1

$$\mathrm{JRC} = \frac{\alpha - \phi_r}{\log \dfrac{\mathrm{JCS}}{\sigma_{no}'}} \quad \text{(2)}$$

in which α = tilt angle when sliding occurs (typically 50°–75°); and σ_{no}' = effective normal stress acting across the joint when sliding occurs.

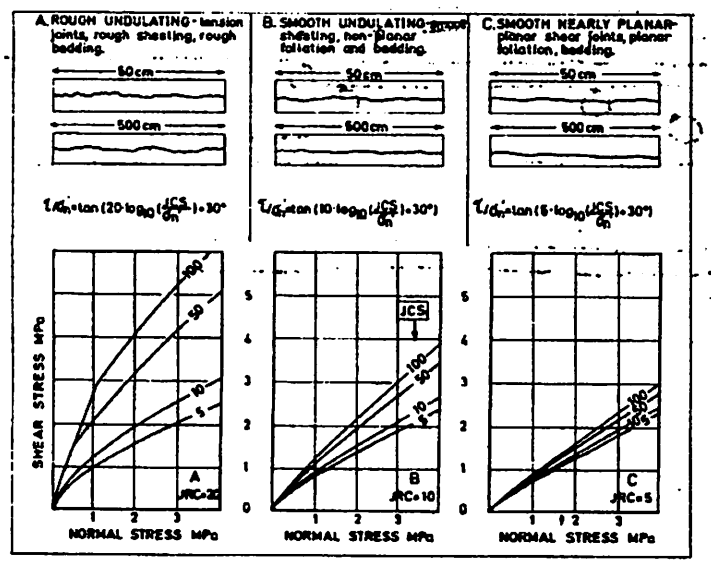

FIG. 1.—Method of Estimating Peak Shear Strength of Rock Joints, Based on Joint Roughness Coefficient JRC (20, 10, or 5), and on Joint Wall Compression Strength JCS (100 MPa, 50 MPa, 10 MPa, or 5 MPa) (2) (1 MPa = 145 psi)

Later in this paper it is shown how an equivalent roughness (R) can be estimated for rockfill, based on the porosity, and on the degree of particle roundedness and surface smoothness. Alternatively, R can be back calculated from large-scale tilt tests of in-place rockfill.

JCS.—Each envelope in Fig. 1 is numbered with the appropriate joint wall compression strength (JCS) value in units of megapascals (1 MPa = 145 psi). The joint wall compression strength can be measured directly with a Schmidt hammer, or estimated from the uniaxial compression strength (σ_c) of the rock. Weathered joints have JCS values less than σ_c, due to the weakening effect of the thin skin of weathered rock along the two walls of the joint. If the joints are saturated, both σ_c (unweathered) and JCS (weathered) are somewhat reduced. This reduction in compression strength due to water saturation is an important factor in explaining the long-term settlement of rockfill dams, as explained by Terzaghi (25) and the second writer (12).

Later in this paper it is shown how an equivalent compression strength (S) can be obtained for rockfill, based on the uniaxial compression strength of the rock and on the d_{50} particle size. Large particles prove to be weaker than smaller ones. A similar scale effect for joint asperities has been demonstrated in recent work reported by Bandis, et al. (1).

ϕ_r and ϕ_b.—The *residual* angle of friction ϕ_r of a rock joint may be reached after large shear displacements when joint asperities are worn down. It is shown as 30° in Fig. 1 for simplicity. In practice, ϕ_r may range from about 15°–30°, depending on the degree of weathering and on the mineralogy of the rock. When joints are unweathered, i.e., JCS = σ_c, the minimum shear strength angle is some degrees higher and is called the *basic* angle of friction ϕ_b. It usually ranges from about 25°–35°. It can be estimated indirectly by conducting simple tilting tests, using dry, flat, nondilatant, i.e., sawn, surfaces of the rock in question. The value of ϕ_b is a fundamental parameter of intact rock, and

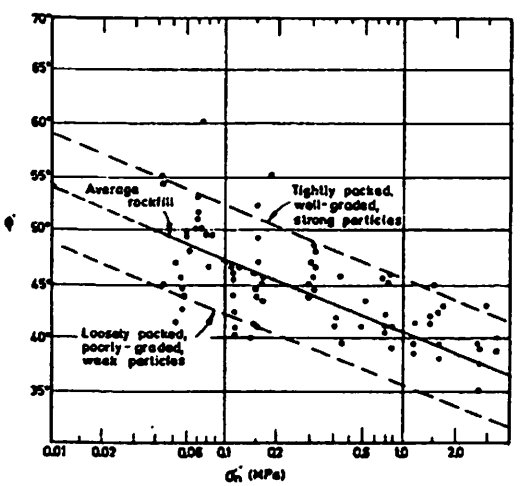

FIG. 2.—Triaxial Test Results for Rockfill (15) (1 MPa = 145 psi)

seems to be a key parameter in describing the shear strength of rockfill.

The *residual* friction angle (ϕ_r) of weathered rock joints is very difficult to determine experimentally, due to the large displacements required. It can nevertheless be estimated with acceptable accuracy by using a Schmidt hammer and tilt test to measure the parameters given in the following empirical relationship:

$$\phi_r = (\phi_b - 20) + 20\left(\frac{r_1}{r_2}\right) \quad (3)$$

in which r_1 = Schmidt (L-type) hammer rebound on saturated weathered joints or interfaces; and r_2 = Schmidt (L-type) hammer rebound on dry, unweathered rock surfaces (for example fresh fractures or sawn surfaces).

As an example, values of $\phi_b = 30°$, $r_1 = 30$, and $r_2 = 40$ result in an estimated $\phi_r = 25°$. Experimental details are described in greater detail by the first writer and Choubey (4).

Comparison with Rockfill Behavior.—Direct shear tests performed on 130 rock-joint specimens selected from seven Norwegian rock types gave the following mean values of these key parameters: (1) JRC = 8.9; (2) JCS = 13,350 psi

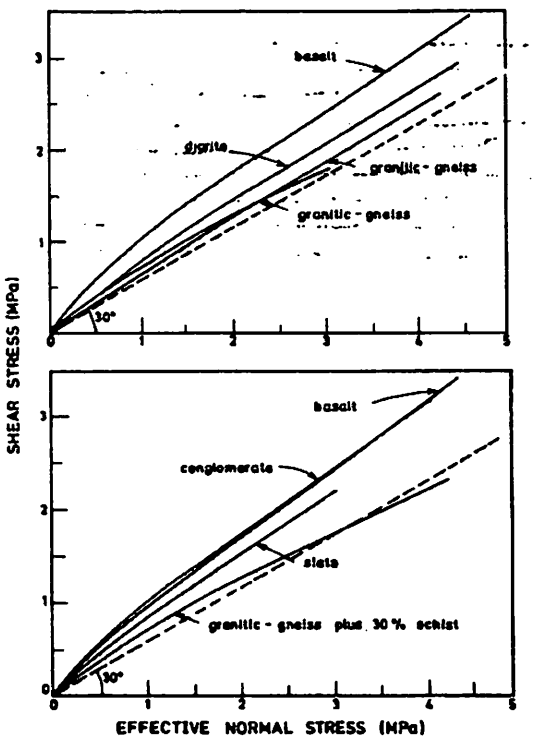

FIG. 3.—Nonlinear Mohr Envelopes for Various Rockfill Materials (19) (1 MPa = 145 psi)

(90 MPa), and (3) $\phi_r = 27.5°$. Eq. 1 shows that the resulting value of ϕ' (= arctan τ/σ'_n) under an effective normal stress of 145 psi (1 MPa) would be 45°.

A review of numerous triaxial tests on rockfill materials by Leps (15) shown in Fig. 2 indicates that "average rockfill" displays a value of ϕ' nearer 40° under the same stress level. The aforementioned rock joints seem to display an average peak shear strength comparable to Leps' "tightly packed, well-graded, strong particles" of rockfill. Note that the log-linear trend of σ'_n versus ϕ' assumed by Leps is also predicted and measured for the case of rock joints (Eq. 1).

Mohr envelopes obtained from triaxial tests on rockfill are nonlinear, and

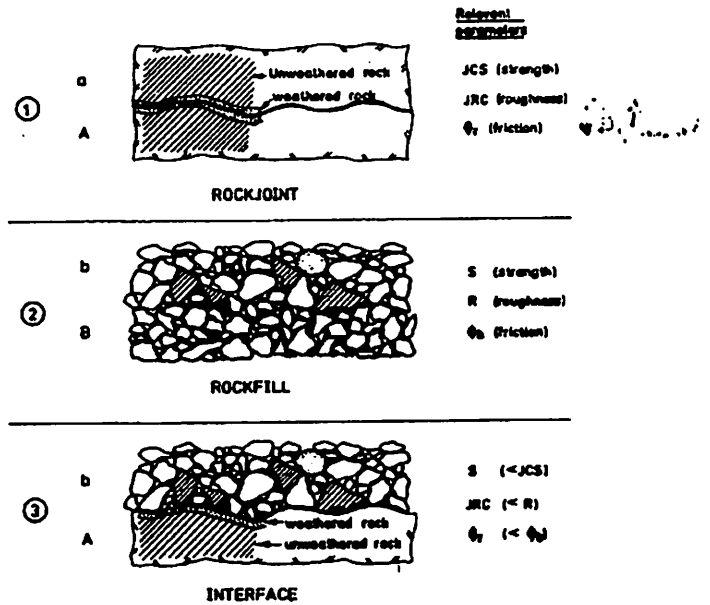

FIG. 4.—Empirical Approach to Shear Strength Estimation for Rock Joints, Rockfill, and Rock Interfaces

very similar in shape to the peak strength envelopes obtained from shear box tests on rock joints. This is clear when comparing Fig. 3 with Fig. 1 (see Class B joints).

A fundamental reason for this similarity of behavior can be found in the observations of contact area during shear tests on rock joints. Shear tests that are interrupted at the instant of peak strength display an apparent visible area (A_1) of damaged asperities that is a small fraction of the total joint sample area (A_0) usually assumed when converting force to stress. The ratio A_1/A_0 is found to be approximately equal to σ'_n/JCS. In other words, compressive failure is occurring at the points of contact at the instant of peak strength, whether the stress is very low, i.e., $A_1/A_0 = 0.001$, or very high, i.e., A_1/A_0

= 0.1. This is similar in principle to the yielding of contact points observed in metal friction.

At extremely high stress JCS increases due to the confining effect caused by A_1 approaching A_0. At this stage the value of JCS is most accurately represented by the triaxial strength $(\sigma_1' - \sigma_3')$ of the rock itself, and substitution of this term in Eq. 1 gives a very accurate fit to high stress data.

The maximum possible shear resistance of rocks occurs when $\sigma_n' \cong \sigma_1' - \sigma_3'$, according to a detailed review of data by the first writer (3). This horizontal point on the Mohr envelope is reached when $\sigma_1' = 3\sigma_3'$, and ϕ' is 30°. By implication, dilation is totally suppressed, $A_1 \cong A_0$, and behavior is essentially ductile.

$d_{max}\uparrow, \phi'\downarrow$

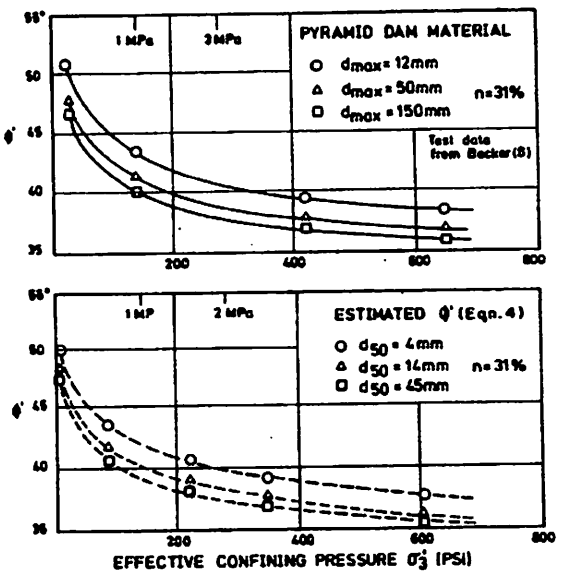

FIG. 5.—Measured Effect of Particle Size on ϕ' (8) and Comparison with Estimated ϕ' Values (1 in. = 25.4 mm)

The apparent link between rock joint and rockfill behavior is seen when triaxial test data are analyzed using the "particle breakage factor" (B). This term was defined by Marsal (18) as the percentage by weight of particles that have undergone crushing following a triaxial shear test. Data collected by Marachi et al. (16) indicate that σ_1'/σ_3' approaches a limiting value of 3.0, and ϕ' approaches a minimum of 30° if the particle breakage factor (B) is extrapolated to 100%. This limiting state cannot be reached unless exceptionally high confining stresses are applied. In practice the particle breakage factor seldom exceeds 40%.

Estimating Shear Strength of Rockfill

The empirical approach to shear strength estimation to be followed in the remainder of this paper is shown diagramatically in Fig. 4. We will be seeking

an equivalent strength of particles (S) and an equivalent roughness (R) to represent as fully as possible the complicated behavior of rockfill. The following form of Eq. 1 is therefore envisaged for rockfill:

$$\phi' = R \cdot \log\left(\frac{S}{\sigma_n'}\right) + \phi_b \quad \text{(4)}$$

Some important aspects of the behavior of rockfill will be summarized to provide a frame of reference for assessing the performance of Eq. 4.

Crushing of Particles: Scale Effects.—Marachi et al. (16,17) and Becker (8) observed that the following factors increased the amount of particle crushing:

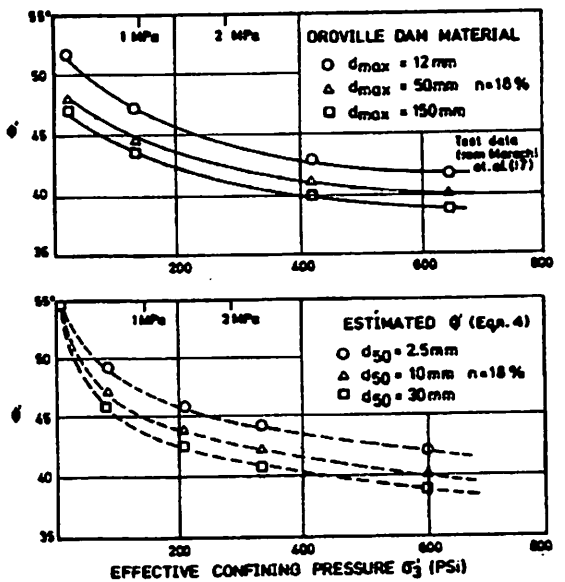

FIG. 6.—Measured Effect of Particle Size on ϕ' (17) and Comparison with Estimated ϕ' Values (1 in. = 25.4 mm)

(1) Increased water content; (2) increased uniformity; (3) increased angularity; (4) reduced particle strength; (5) increased effective confining pressure (σ_3'); (6) increased shear stress under a given confining pressure; (7) testing in a triaxial cell as compared to plane strain testing; and (8) increased particle sizes.

Reduced shear strength with increased particle size is a particularly well documented result for rockfill, following the detailed studies at the University of California, Berkeley. Some of the results of these scale effect investigations are reproduced in the upper half of Figs. 5 and 6. The experimental data incorporates d_{50} particle sizes ranging from 0.08 in.–1.8 in. (2 mm–45 mm) using triaxial cells with diameters ranging from 2.8 in.–36 in. (70 mm–910 mm).

Scale effects appear to be marked in this range of particle sizes but apparently die out at either end. For example, triaxial tests reported by Vallerga, et al.

(26) indicated no noticeable scale effects for samples with d_{max} less than 0.2 in. (5 mm), and crushing tests on single sand grains with diameters from 0.016 in–0.075 in. (0.4 mm–2 mm) reported by Billam (9) suggest limited scale effect for sand below 0.028 in. (0.7 mm) size.

An upper bound is suggested in a comprehensive review for uniaxial compression test data for rock reported by Lama and Gonano (14). For the most part, rock samples with volumes larger than 10 L (610 cu in.) displayed a relatively insignificant scale effect, while smaller samples displayed considerable scale effect. The statistical volume theory of Weibull (27) appears to be the explanation for these effects. The probability of a sample containing microfractures increases as the volume increases. The fact that the larger rock samples may contain numerous microfractures and sand grains probably none, is perhaps the reason for the S-shaped relation between crushing strength and particle size shown in Fig. 7.

In the light of the preceding it appears logical to introduce a size-dependent equivalent strength (S) for rockfill. This would be consistent with scale effects

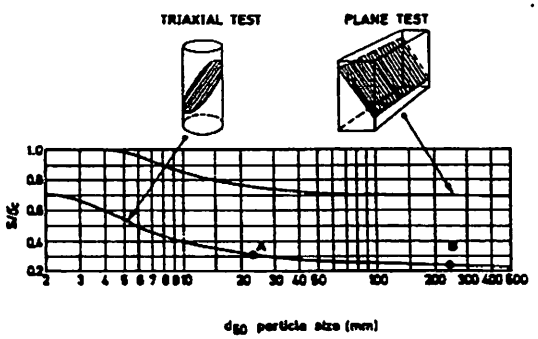

FIG. 7.—Method of Estimating Equivalent Strength (S) of Rockfill, Based on Uniaxial Compression Strength (σ_c), and on d_{50} Particle Size

observed from shear tests of rock joints. Bandis et al. (1) demonstrate how the joint wall compression strength (JCS) reduces with increasing size of joint sample, due to the mobilization of larger asperities at peak strength. Larger displacements are required to reach peak strength, as the length of sample is increased.

Trial and error fitting of numerous triaxial data with our prediction model (Eq. 4) has led to the empirical solution to particle size effects shown in Fig. 7. It should be noted that the d_{50} size will not necessarily be the most relevant particle size for estimating the equivalent strength (S) of a given grading. The d_{50} size is however a convenient description of a given rockfill. Shear strength differences between a widely and narrowly graded rockfill with equal d_{50} sizes will presumably arise chiefly from the different porosities attainable, and this will affect the structural component of strength independent of any possible changes of equivalent particle strength (S).

The example points A and B on the triaxial test curve in Fig. 7 represent

d_{50} sizes of 23 mm (1 in.) and 240 mm (9.5 in.), respectively. These can be considered representative of laboratory samples and in-place rockfill, respectively. The following equivalent strengths (S) would be appropriate if the uniaxial compressive strength (σ_c) of the parent rock was found to be 150 MPa (21,800 psi): (1) Grading A, d_{50} = 23 mm, $S \cong 150 \times 0.3 = 45$ MPa (6,500 psi); and grading B, d_{50} = 240 mm, $S \cong 150 \times 0.2 = 30$ MPa (4,350 psi).

The great majority of shear-test data for rockfill have been obtained from triaxial testing. However, plane-strain tests are more representative of the strain conditions for many practical situations. It is a common experience with such

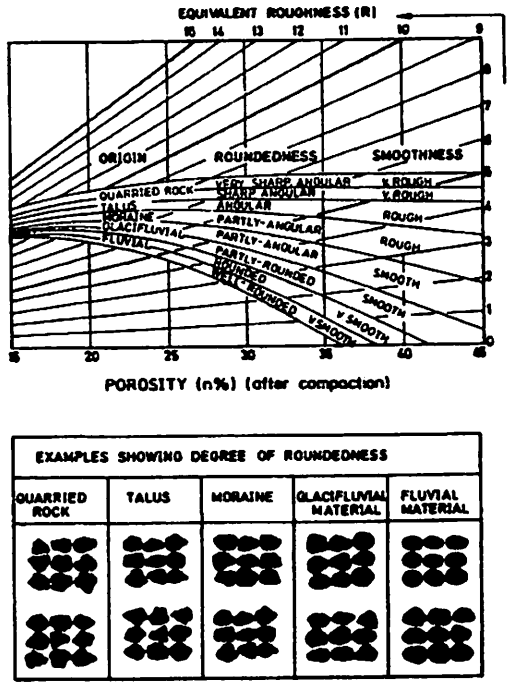

FIG. 8.—Method of Estimating Equivalent Roughness (R) Based on Porosity of Rockfill, Origin of Materials, and Degree of Roundedness and Smoothness of Particles

tests that failure occurs at relatively small strains, that less crushing of particles occurs, and that ϕ' values are at least 2°–4° higher than is the case for triaxial tests on the same materials. The different scale effects for triaxial and plane-strain tests envisaged in Fig. 7 is an empirical but effective method of accounting for these differences in ϕ'. The proposed method will generally result in about 2°–4° differences in ϕ', over the range of stresses of interest.

Degree of Particle Roundedness.—The cohesionless materials used in a rockfill dam will generally come from one or more of the following sources: (1) Quarried rock; (2) talus; (3) moraine; (4) glacifluvial deposits; and (5) fluvial deposits.

Each of these potential sources produced a characteristic degree of particle roundedness and surface smoothness, which in general is dependent on the length of transport from the source of origin. However, the mineralogy of the rocks in question sometimes complicates attempts to correlate length of transport with the degree of roundedness. Softer rocks obviously attain rounded edges more rapidly than hard rocks if both are transported equal distances.

Investigations by Pellegrino (21) nevertheless indicate that particles originating from talus are generally angular, those from glacial deposits are partly angular or partly rounded, and those from fluvial deposits are rounded or well rounded. Morris (20) was able to induce a degree of roundedness artificially by tumbling crushed particles of basalt in water over a long period. The value of ϕ' measured in a special tilt apparatus thereby reduced from 53.8°–46.2°.

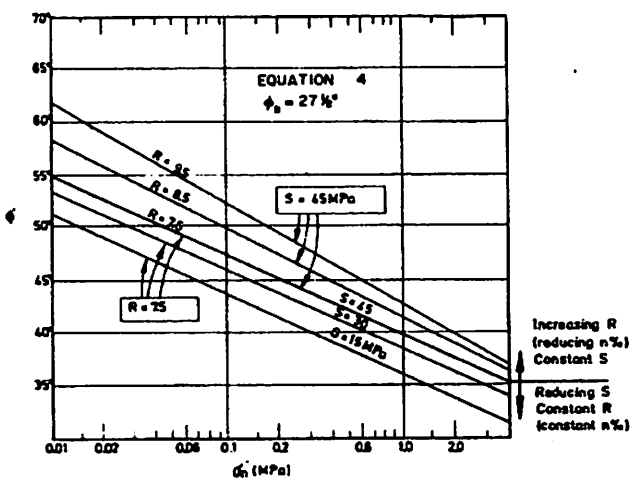

FIG. 9.—Effect of Variable R and S on Shear Strength Estimates [Compare Fig. 2 (15)] (1 MPa = 145 psi)

Several classification systems for particle shape and roundedness have been suggested in the past. Those by Krumbein (13), Powers (23), and Pittijohn et al. (22) were conveniently reviewed by Chilingarian et al. (10). The classification system presented in Fig. 8 combines several aspects of these writers' work, but it is specifically tailored to rockfill rather than sand particles. The addition of porosity (n) and equivalent roughness (R) make it possible to estimate the peak drained friction angle ϕ' of a given rockfill, using Eq. 4. The method was developed through trial and error, by backanalysis of numerous triaxial (and some plane strain) tests on rockfill materials reported in the literature. Unpublished data from tests at the Norwegian Geotechnical Institute were also included.

Example Applications of Equivalent Roughness Method.—The aforementioned method for estimating the peak strength of rockfill requires the following input:

d_{50} particle size σ_c uniaxial compressive strength of rock	equivalent strength (S) (Fig. 7)
description: origin roundedness smoothness n% porosity after compaction	equivalent roughness (R) (Fig. 8)
ϕ_b basic friction angle	(usual range 25°–35°)

Figs. 5 and 6 show the potential of the method. Estimated ϕ' values, and their variation with confining pressure and particle size, are compared with measured data for Pyramid dam argillite (quarried rock) and Oroville dam amphibolite (fluvial gravel). Uniaxial compression strengths were 15,805 psi (110 MPa) and 28,565 psi (200 MPa), respectively.

TABLE 1.—ϕ' Varies by R Degrees for Each Ten-Fold Change in Pressure

σ_n', in megapascals (1)	Equivalent overburden (2)	ϕ' plane (3)	ϕ' triaxial (4)
0.0001	5 mm	67°	65°
0.001	50 mm	61°	59°
0.01	500 mm	55°	53°
0.1	5 m	49°	47°
1.0	50 m	43°	41°
10.0	500 m	37°	35°

Note: 25.4 mm = 1 in.; 1 MPa = 145 psi.

It is interesting to return to the log-linear plot of σ_n' versus ϕ' for rockfill, shown in Fig. 2. We can now study the effects of variations in porosity and rock strength on ϕ', since these variables have a direct effect on R and S, respectively. In Fig. 9 some typical values of R and S are plotted by evaluating Eq. 4 with ϕ_b = 27.5°. The "tightly packed, well graded, strong particles" in Fig. 2 are readily simulated by high values of R and S, while low values of both parameters provide the best fit to the "loosely packed, poorly-graded, weak particles." It appears that Leps was correct in drawing straight line envelopes (ϕ' inversely proportional to $\log \sigma_n'$), but he may have been incorrect in drawing parallel upper and lower envelopes.

Shear Strength of Rockfill under Extremely Low Stress.—The triaxial data reviewed by Leps (15) included no tests with σ_n' less than about 0.04 MPa (6 psi). Yet even lower values operate at the toe and close to the face of a rockfill dam. The associated high values of ϕ' are probably responsible for the extremely favorable resistance to ravelling. Accurate determination of ϕ' under extremely low values of σ_n' is clearly of practical interest.

Special plane-strain shear box tests on angular particles of crushed granite

reported by Seed and Goodman (24) indicated values of ϕ' as high as 67°, under an effective normal stress of approximately 10^{-4} MPa (0.0145 psi).

Extremely high ϕ' values are also predicted by the equivalent roughness method (Eq. 4) at these low stress levels. If we assume the following input data as representative of Seed and Goodman's crushed granite: d_{50} = 7.5 mm (0.3 in.); σ_c = 150 MPa (21,750 psi); n = 35%; and ϕ_b = 30°, the results presented in Table 1 are obtained. The equivalent roughness (R) of six in this example is obtained from Fig. 8, based on assumed "sharp, angular very rough particles" of crushed granite. The predicted values of ϕ' appear to be realistic over five orders of magnitude of stress, judging by the high stress data shown in Figs. 5 and 6.

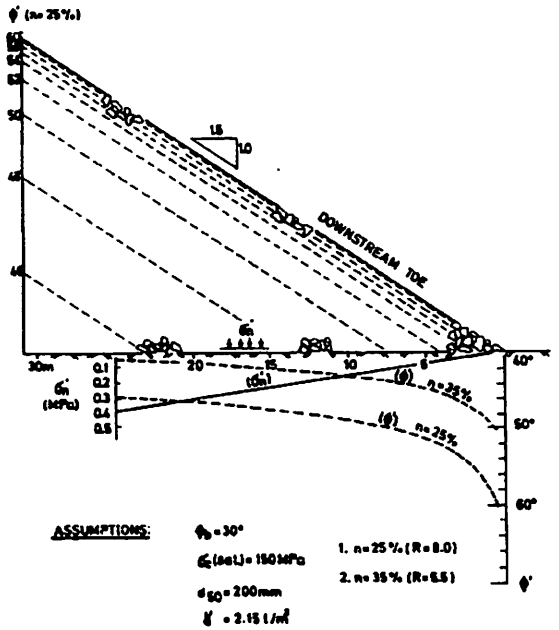

FIG. 10.—Estimated Variation of ϕ' under Toe and beneath Downstream Slope of Dam

The triangular shape of rockfill dams results in approximately triangular self-weight vertical stress distributions, and correspondingly high ϕ' values close to the toe, as shown in Fig. 10. Values of ϕ' in excess of 50° and 60° are estimated for the assumed porosities of 35% and 25% in these examples. It is also interesting to see the high values of ϕ' close to the downstream face of the dam. If this slope was analyzed as an infinitely long slope, with safety factor $F = \tan\phi'/\tan\theta$ (in which θ = slope angle), then it is clear that F would be quite high close to the face.

Variation of Mobilized ϕ' with Deformation.—While the main purpose of this

paper is the estimation of peak ϕ' for rockfill, it is clear that the strain required to mobilize peak strength is also of considerable importance.

An analysis of some forty triaxial tests has indicated a relationship between ϵ_{peak} (the axial strain at peak strength), and $(\phi' - \phi_b)$. The latter can be termed the structural component of strength (i), in which

$$i = R \log\left(\frac{S}{\sigma'_n}\right) \quad (5)$$

The test data analyzed indicated the following approximate ranges of ϵ_{peak}, as a percentage: Maximum $\epsilon_{peak} \cong 20\text{-}2/3\,(\phi' - \phi_b)$ for $n > 30\%$; and minimum $\epsilon_{peak} \cong 10\text{-}1/3\,(\phi' - \phi_b)$ for $n < 20\%$.

Thus a general relationship for axial strain at peak is the following:

$$\epsilon_{peak} \cong 1/30\,(n - 10)(30 - i)(\%) \quad (6)$$

The following example illustrates a typical case:

quarried granite, n = 28% } R = 7.5

σ_c = 21,750 psi (150 MPa), d_{50} = 0.8 in. (20 mm) } S = 7,250 psi (50 MPa)

ϕ_b = 30°

σ_n = 72.5 psi (0.5 MPa)

Eqs. 5 and 6 give i = 15°, ϕ' = 45°, ϵ_{peak} = 9.0%.

TABLE 2.—Mobilization of Equivalent Roughness (R) of Rockfill with Increasing Axial Strain (ϵ_{inst} = Axial Strain at Any Instant)

$\epsilon_{inst}/\epsilon_{peak}$ (1)	R_{mob}/R_{peak} (2)
0	$-\phi_b/i$
0.25	0.25
0.50	0.75
1.00	1.00

Note: $i = (\phi' - \phi_b) = R_{peak} \cdot \log(S/\sigma'_n)$.

The mobilization of shear strength as rockfill is strained towards peak shear strength can be characterized by the term R_{mob}. Thus, the friction angle mobilized at any given strain may be expressed as:

$$\phi'_{mob} = R_{mob} \cdot \log\left(\frac{S}{\sigma'_n}\right) + \phi_b \quad (7)$$

This concept was used by Barton (6) to generate shear stress displacement curves for rock joints for any desired loading or unloading. In the case of

rock joints the term JRC_{mob} was used. Table 2 shows how even an extremely simple table of values can be used to generate realistic stress-strain or ϕ'_{mob}-strain curves for rockfill.

An example application of this method is shown in Fig. 11. Measured data derived from vacuum triaxial tests at the Norwegian Geotechnical Institute (Janbu, 11) are compared with estimated data. Two different gradings are investigated, one representing the laboratory tests with d_{50} = 6 mm (0.24 in.), the other (stippled) representing the grading in the dam where d = 250 mm (9.8 in.) Realistic values of σ_c (saturated) = 150 MPa (21,750 psi) and ϕ_b = 25° were assumed for the schistose gneiss. Note the reduced strength and increased deformability predicted for the full-scale material. The important influence of

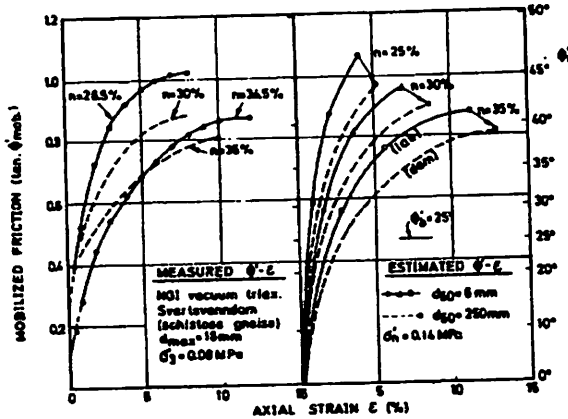

FIG. 11.—Comparison of Measured and Estimated Mobilization of ϕ' with Increasing Axial Strain (1 MPa = 145 psi, 1 in. = 25.4 mm)

compaction, i.e., porosity, on strength and deformability is clearly reflected in both the measured and estimated results.

Practical Applications

The proposed method for estimating the peak strength of rockfill requires the following input:

- d_{50} particle size
- σ_c uniaxial compressive strength of rock

} equivalent strength S (Fig. 7)

- description of rockfill: origin, roundedness, smoothness
- n% porosity after compaction
- ϕ_b basic friction angle

} equivalent roughness R (Fig. 8)

The value of σ_c can be estimated from simple index tests such as the Schmidt hammer or point load test. The value of ϕ_b can be estimated from tilt tests of sawn surfaces of the rock in question. It usually ranges from 25°–35°, depending on rock type.

Preliminary Parametric Studies.—The equivalent roughness method is recommended for obtaining preliminary estimates of ϕ', prior to detailed strength investigations. A particular advantage is the ease with which parametric studies can be performed. Shear strength envelopes can be generated from Eq. 4 to investigate the effects of varying the particle size, varying the compactive effort, or varying the type of rockfill. Eq. 7 and Table 2 can be used to generate approximate mobilized friction/axial strain curves.

Extrapolation of Laboratory Shear Strength Data.—During the more detailed strength investigation that usually precedes construction of a rockfill dam, the

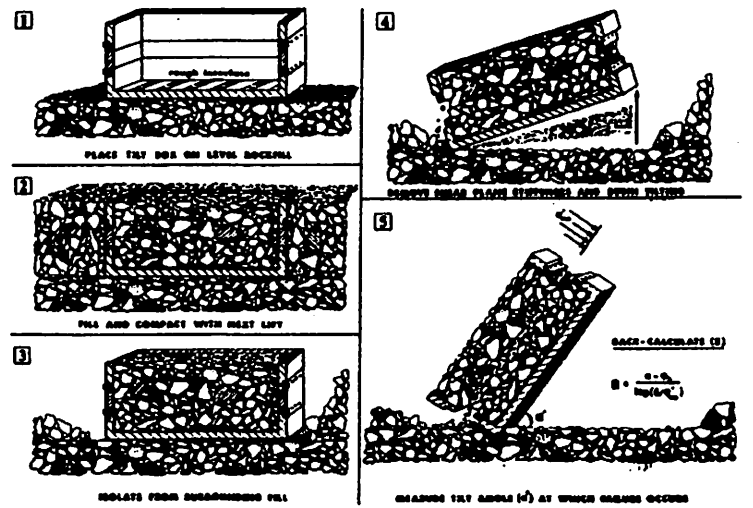

FIG. 12.—Method for Checking Full-Scale Strength (and Porosity) of Different Lifts in Dam or Trial Fill

method can be used to extrapolate triaxial (or plane strain) strength data to stress levels above and below those normally employed. This will be particularly advantageous for the case of large vacuum triaxial tests. In general, it is recommended that the equivalent roughness (R) is back calculated from the available test data, and the values of S and ϕ_b estimated from simple index tests. However, there may be occasions when Fig. 8 is considered adequate for estimating (R), and therefore the value of equivalent particle strength (S) would be back calculated as a basis for extrapolating available test data. The assumed dependency of ϕ' on the d_{50} particle size, which is an obvious simplification, would then be unnecessary. Equivalent particle strength (S) would be back calculated by rearrangement of Eq. 4. Thus

$$S = \sigma'_n \cdot 10^{(I/R)} \quad \text{(8)}$$

Extrapolation of Large-Scale Tilt Tests of In-Place Rockfill.—A serious limitation of laboratory shear strength investigations is the inability to test full-scale rockfill samples with as-built gradings and porosities. Development of this equivalent roughness method, with its apparent abilities for accurate extrapolation of strength over many orders of magnitude of stress, has provided a means of interpreting large-scale tests performed under extremely low stress.

In practice, a robust rectangular open box split horizontally could be placed on a trial fill or on the partly completed dam, ready for sampling the next lift of rockfill. It would be embedded, filled, and compacted by the customary number of passes of a vibrating roller. Subsequent excavation of fill from around the outsides of the box would release it and allow the whole box, preferably several meters in length, to be lifted hydraulically at one end. Fig. 12 shows the principle.

The maximum angle of tilt ($\alpha°$) tolerated before failure, would probably be of the order of 55°–65° under the extremely low effective normal stress operating across the failure surface. The angle $\alpha° = \phi'$ would be extrapolated to design stresses by estimating values of S and ϕ_b from index tests, and back calculating the value of R from Eq. 4. Note that errors in estimating S and ϕ_b are automatically compensated by the values of R back calculated. Tilt tests have the added advantage that the nonuniform strain and progressive failure common to conventional shear box tests is much reduced, due to the inherently more uniform nature of gravitationally induced shear and normal stress.

An important by-product of the test would be the relative ease with which in-place porosity could be measured. This would be calculated from the known volume of the tilt sample, and from the force required to lift one end, i.e., one half, of the tilt box, before and after filling.

Summary and Conclusions

1. Shearing between the two interlocked walls of a rock joint, or between the interlocked particles of a rockfill, involves a significant degree of overriding (dilation) under low effective stress and a significant degree of crushing of contact points under high effective stress. The peak shear strength of the two materials is surprisingly similar, although rock joints generally reach their peak strength at much smaller strains than rockfill.

2. The peak drained friction angles of rock joints and rockfill can be quantified by an equivalent roughness (JRC or R), an equivalent asperity or particle compression strength (JCS or S), and by the residual or basic friction angle (ϕ_r or ϕ_b), respectively. The latter are generated by nondilatent surfaces of the given rock types. Each of these six parameters can be estimated by simple index tests, or by classification. In the case of rockfill, the porosity, the degree of particle roundedness, the d_{50} size, and the uniaxial compression strength of the relevant rock are all essential to the estimation of ϕ', the peak drained friction angle.

3. The value of ϕ' for both rockfill and rock joints is found to be inversely proportional to the log of effective normal stress. Thus ϕ' for rockfill increases by some 4°–8° for each ten-fold reduction in effective normal stress. Extremely high values of ϕ' are observed for very low effective stress levels. This stress dependency is a very positive factor in the critical toe region of a rockfill dam. High ϕ' values in this region help to explain the high resistance to ravelling during extreme leakage.

4. The satisfactory fit between estimated and measured ϕ' values over several orders of magnitude of stress, suggest that large-scale tilt testing of in-place compacted rockfill may be a promising economic method of checking full-scale strength and porosity in different lifts of a dam, or in a trial fill prior to dam construction.

Acknowledgments

The writers are grateful to Kaare Høeg for reading the original manuscript and for significantly reducing its length to the advantage of reader and writer alike.

Appendix I.—References

1. Bandis, S. Barton, N., and Lumsden, A., "Experimental Studies of Scale Effects on the Shear Behavior of Rock Joints," *International Journal of Rock Mechanics, Mining Sciences and Geomechanics Abstracts*, Vol. 18, 1981, pp. 1–21.
2. Barton, N., "Review of a New Shear Strength Criterion for Rock Joints," *Engineering Geology*, Vol. 7, 1973, pp. 287–332.
3. Barton, N., "The Shear Strength of Rock and Rock Joints," *International Journal of Rock Mechanics, Mining Sciences and Geomechanics Abstracts*, Vol. 13, No. 9, 1976, pp. 255–279.
4. Barton, N., and Choubey, V., "The Shear Strength of Rock Joints in Theory and Practice," *Rock Mechanics*, Springer-Verlag, Austria, Vol. 10, No. 1/2, 1977, pp. 1–54.
5. Barton, N., and Bandis, S., "Some Effects of Scale on the Shear Strength of Joints," *International Journal of Rock Mechanics, Mining Sciences and Geomechanics Abstracts*, Technical Note, Vol. 17, 1980, pp. 69–73.
6. Barton, N., "Estimation of In-Situ Joint Properties, Naslinden Mine," *Proceedings of the Lulea Conference on Application of Rock Mechanics to Cut-and-Fill Mining*, Society of Mining Engineers, London, England, 1980.
7. Barton, N., "Vurdering av Skjaerfasthet i Steinfyllinger of Mellom Steinfylling og Fjellfundament," *Internal Report*, No. 53101-2, Norwegian Geotechnical Institute, Oslo, Norway, 1980, p. 67.
8. Becker, E., "Strength and Deformation Characteristics of Rockfill Materials Under Plane Strain Conditions," thesis presented to the University of California, at Berkeley, Calif., in 1972, in partial fulfillment of the requirements for the degree of Doctor of Philosophy.
9. Billam, J., "Some Aspects of the Behavior of Granular Materials at High Pressures," *Proceedings of the Roscoe Memorial Symposium*, 1971, pp. 69–80.
10. Chilingarian, G. V., Wolf, K. H., and Allen, D. R., "Introduction, Compaction of Coarse-Grained Sediments," G. V. Chilingarian and K. H. Wolf, eds., Elsevier Publishing Co., Inc., Amsterdam, Holland, Vol. 1, 1975, pp. 1–42.
11. Janbu, N., "Svartevannsdammen; Stabilitet av Nedstrøms Støttefying," *Report*, Sira-Kvina Kraftselskap, 1974.
12. Kjaernsli, B., "Earth and Rock Dams, Slopes and Open Excavations," *Proceedings*, International Conference on Soil Mechanics and Foundation Engineering, Vol. 3, 1965, pp. 570–573.
13. Krumbein, W. C., "Measurement and Geologic Significance of Shape and Roundness of Sedimentary Particles," *Journal of Sedimentary Petrology*, Vol. 11, 1941, pp. 64–72.
14. Lama, R. D., and Gonano, L. P., "Size-Effect Considerations in the Assessment of Mechanical Properties of Rockmasses," presented at the 1976 Symposium on Rock Mechanics, held at Dhanbad, India.
15. Leps, T. M., "Review of Shearing Strength of Rockfill," *Journal of the Soil Mechanics*

and Foundations Division, ASCE, Vol. 96, No. SM4, Proc. Paper 7394, July, 1970, pp. 1159–1170.

16. Marachi, N. D., Chan, C. K., Seed, H. B., and Duncan, J. M., "Strength and Deformation Characteristics of Rockfill Materials," Department of Civil Engineering, University of California, Berkeley, Calif., 1969, 139 p.
17. Marachi, N. D., Chan, C. K., and Seed, H. B., "Evaluation of Properties of Rockfill Materials," *Journal of the Soil Mechanics and Foundations Division*, ASCE, Vol. 98, No. SM1, Proc. Paper 8672, Jan., 1972, pp. 95–114.
18. Marsal, R. J., "Soil Properties, Shear Strength and Consolidation," *Proceedings*, International Conference on Soil Mechanics and Foundation Engineering, Vol. 3, 1965, pp. 310–316.
19. Marsal, R. J., "Mechanical Properties of Rockfill," *Embankment-Dam Engineering, Casagrande Volume*, R. C. Hirshfeld and S. J. Poulos, eds., John Wiley and Sons, Inc., New York, N.Y., 1973, pp. 109–200.
20. Morris, H. C., "Effect of Particle Shape and Texture on the Strength of Non-Cohesive Aggregates," *Special Technical Publication*, American Society for Testing and Materials, No. 254, 1959, pp. 350–364.
21. Pellegrino, A., "Geotechnical Properties of Coarse-Grained Soils," *Proceedings*, International Conference on Soil Mechanics and Foundation Engineering, Vol. 1, 1965, pp. 87–91.
22. Pettijohn, F. J., Potter, P. E., and Siever, R., *Sand and Sandstone*, Springer, New York, N.Y., 1972, 618 p.
23. Powers, M. C., "A New Roundness Scale for Sedimentary Particles," *Journal of Sedimentary Petrology*, Vol. 23, 1953, pp. 117–119.
24. Seed, H. B., and Goodman, R. E., "Earthquake Stability of Slopes of Cohesionless Soils," *Journal of the Soil Mechanics and Foundations Division*, ASCE, Vol. 90, No. SM6, Proc. Paper 4128, Nov., 1964, pp. 43–73.
25. Terzaghi, K., discussion of "Rockfill Dams: Salt Springs and Lower Bear River Concrete Face Dams," by J. C. Steele and J. B. Cooke, *Journal of the Power Division*, ASCE, Vol. 86, No. PO1, Proc. Paper 2392, Feb., 1960, pp. 65–74.
26. Vallerga, B. A., Seed, H. B., Monismith, C. L., and Cooper R. S., "Effect of Shape, Size and Surface Roughness of Aggregate Particles on the Strength of Granular Materials," *Special Technical Publications*, American Society for Testing and Materials, No. 212, 1957, pp. 63–74.
27. Weibull, W., "A Survey of Statistical Effects in the Field of Material Failure," *Applied Mechanics Review*, Vol. 5, 1952, pp. 449–451.

Appendix II.—Notation

The following symbols are used in this paper:

A_1 = apparent (visible) area of damaged asperities when rock joint is sheared up to peak strength;
A_0 = total area of rock joint sample assumed when converting force to stress;
B = particle breakage factor after Marsal (18);
d_{max} = maximum particle size;
d_{50} = particle size with 50% passing;
F = safety factor;
i = structural component of shear strength for rockfill, where $i = \phi' - \phi_b$;
JCS = joint wall compression strength;
JRC = roughness coefficient of rock joints;
n = porosity, as a percentage (after compaction);
R = equivalent roughness of rockfill;

r_1 = Schmidt (L) hammer rebound number, measured on saturated, weathered joints;
r_2 = Schmidt (L) hammer rebound number, measured on dry, unweathered rock surfaces;
S = equivalent strength of rockfill particles;
$\alpha°$ = maximum angle of inclination recorded when upper half of jointed block of rock (or rockfill sample) slides under influence of gravity loading, during tilt test;
ϵ = axial strain, as a percentage;
σ_c = uniaxial compression strength measured on cylindrical rock samples;
σ'_n = effective normal stress;
σ'_{no} = effective normal stress acting when sliding occurs during tilt test;
σ'_1 = effective major principle stress;
σ'_3 = effective confining pressure (applied in triaxial test);
τ = peak shear strength;
ϕ_b = basic friction angle of smooth, planar unweathered rock surfaces;
ϕ_r = residual friction angle of weathered rock joints; and
ϕ' = peak drained friction angle (for rock joints or rockfill).

Subscripts

mob = mobilized value (of R, JRC or ϕ') at any given strain or shear displacement;
inst = instantaneous value (of axial strain ϵ); and
peak = value at peak strength (of ϵ or R).